nature biotechnology

FRET imaging

Elizabeth A Jares-Erijman[1] & Thomas M Jovin[2]

Förster (or Fluorescence) Resonance Energy Transfer (FRET) is unique in generating fluorescence signals sensitive to molecular conformation, association, and separation in the 1–10 nm range. We introduce a revised photophysical framework for the phenomenon and provide a systematic catalog of FRET techniques adapted to imaging systems, including new approaches proposed as suitable prospects for implementation. Applications extending from a single molecule to live cells will benefit from multidimensional microscopy techniques, particularly those adapted for optical sectioning and incorporating new algorithms for resolving the component contributions to images of complex molecular systems.

Biological phenomena are based on the fundamental physico-chemical processes of molecular binding, association, conformational change, diffusion and catalysis. The structural hierarchy established at the level of organelles, cells, tissues and organisms is imposed via an extensive network of cascade and feedback mechanisms based on these reactions. Thus, in order to perform 'biochemistry in the cell' it is imperative to elucidate the spatio-temporal distributions and functional states of the constituent molecules. Fluorescence microscopy is ideally suited to this task because it generates contrast by exploiting the many manifestations of light emission: sensitivity, selectivity, and modulation via reactions in the ground and excited electronic states. Of these, FRET (for a discussion of nomenclature, see Table 1.1 in ref. 1) is unique in providing signals sensitive to intra- and intermolecular distances in the 1–10 nm range. Thus, FRET is capable of resolving molecular interactions and conformations with a spatial resolution far exceeding the inherent diffraction limit (~λ/2) of conventional optical microscopy, yet is also compatible with super-resolution techniques.

This report is intended primarily as a guide to FRET in the imaging environment, although most of the concepts are applicable to solution studies as well. Space limitations preclude a survey of applications, for which the reader is referred to recent reports and reviews[2–11]. We present a somewhat revised formalism for the FRET phenomenon that offers certain advantages over standard analyses and provide a systematic classification of 22 different FRET methods (see also ref. 11). These include several new approaches of potential utility in the research and biotechnological laboratories. We conclude with a brief discussion of selected probe issues and anticipated future developments extending from single molecule to live cell applications.

Fluorescence resonance energy transfer

FRET is a process in which energy is transferred nonradiatively (that is, via long-range dipole-dipole coupling) from a fluorophore in an electronic excited state serving as a donor, to another chromophore or acceptor. The latter may, but need not, be fluorescent. Recent monographs[1,9,10,12,13] and two reviews by R. Clegg[14,15] provide excellent and extensive coverage of this topic.

The transfer rate k_t (see **Box 1** for definitions and basics) varies inversely with the 6th power of the donor-acceptor separation (r^6) over the range of 1–10 nm, as first demonstrated with peptides 40 years ago[16]. Such distances are relevant for most biomolecules or their constituent domains engaged in complex formation and conformational transition. The transfer rate also depends on three parameters: (i) the overlap of the donor emission and acceptor absorption spectra (parameter: overlap integral J); (ii) the relative-orientation of the donor absorption and acceptor transitions moments (parameter: κ^2, range 0–4); and (iii) the refractive index (parameter: n^{-4}, range ≅ 1/3–1/5).

The quantitative treatment of FRET originated with Theodor Förster and is embodied in widely disseminated formulas for k_t, the 'Förster constant' R_o, and the transfer quantum yield generally denoted as the energy transfer efficiency E (equation (1)).

$$k_t = \frac{1}{\tau_o}(R_o/r)^6;\ R_o^6 = c_o\kappa^2 J n^{-4} Q_o = c_o\kappa^2 J n^{-4}(k_f\tau_o);\ E = k_t\tau = \frac{(R_o/r)^6}{1+(R_o/r)^6};$$
$$\tau_o^{-1} = k_f + k_{nr} + k_{isc} + k_{pb};\ \tau^{-1} = \tau_o^{-1} + k_t \qquad (1)$$

where $c_o = 8.8 \times 10^{-28}$ for R_o in nm and $J = 10^{17} \int q_{d,\lambda}\,\varepsilon_{a,\lambda}\lambda^4 d\lambda$ in nm^6 mol^{-1}; $q_{d,\lambda}$ is the normalized donor emission spectrum. As shown in equation (1), the unperturbed lifetime of the donor, τ_o, appears both in the denominator and in the numerator (second expression for R_o^6). Thus, upon canceling terms one is left only with the radiative rate constant k_f in the numerator. This quantity reflects inherent properties of the fluorophore, including solvation, and can generally be regarded as invariant under given experimental conditions[13,17]. It follows that the fundamental relationship established by Förster between k_t and k_f bears no necessary relationship to the reference donor lifetime τ_o or to the derived quantum yield Q_o. That is, the inclusion of these quantities in the definition of R_o is arbitrary, and justified only because most, but not all, estimations of the transfer efficiency (E) are made by comparisons with the properties of the unperturbed donor. (It is interesting that in his widely cited English review[18], Förster made no mention of R_o,

[1]Departamento de Química Orgánica, Facultad de Ciencias Exactas y Naturales, Universidad de Buenos Aires, 1428 Buenos Aires, Argentina. [2]Department of Molecular Biology, Max Planck Institute for Biophysical Chemistry, 37077 Göttingen, Germany. Correspondence should be addressed to E.A.J.-E. (eli@qo.fcen.uba.ar) or T.M.J. (tjovin@gwdg.de).

Published online 31 October 2002; doi:10.1038/nbt896

although he commented on the remarkable absence of Planck's constant from $n_{a\to b}$, his expression for k_t.)

A major problem with cell biological applications of FRET, particularly those involving imaging techniques, is that the reference value τ_o is generally unknown and may vary continuously and arbitrarily throughout the sample, for example as a result of changes in the generally environment-sensitive k_{nr}. In addition, although the donor-separation distance r is of primary interest in most FRET experiments, one or more of the other parameters incorporated in the definition of R_o may also change or be of even greater functional significance. Possible examples would be molecular translocations between the cytoplasm and the plasma membrane, and conformational rearrangements. Of central relevance in the latter instance is the orientational factor, κ^2, to which one almost universally assigns the value of 2/3. Unfortunately, this procedure is valid only if the donor and acceptor molecules are oriented randomly and rotate rapidly and isotropically during the donor excited-state lifetime. Such a condition may often or generally fail to exist, as with the visible fluorescent proteins (VFPs), the rotational correlation times (see below) of which are ~fivefold their lifetimes, thereby greatly limiting the extent of rotational relaxation[19,20]. (It follows that R_os reported for the various VFPs (ref. 21) must be used with caution.) For a random yet static molecular distribution, the ensemble κ^2 is not even a constant but

Table 1 Methods for determining FRET in fluorescence microscopy

Category	Method	Resonance energy transfer parameters	References
I. Donor quenching and/or acceptor sensitization			
Ia. Combined donor (D) and acceptor (A) emission signals			
Ia1	2,3 signals; spectra	Calibrated functions	3,11,14,15,36,50,66–69
Ia2	Normalized D/A ratio	$\theta = Q_a R_{da}$; $R_{da} \propto I^d_{da,d}/I^a_{da,d}$	67,70
Ia3	Bioluminescence RET (BRET)	$\theta \propto I_b/I_a$	71
Ib. Fluorescence-detected excited state lifetime(s) (FLIM)			
Ib1	D lifetime	$\rho = \tau/\tau_o$	2,9,17,31,63,72–83
Ib2	Luminescence RET (LRET)	$\rho = \tau^a_{da,d}/\tau_o$	70
Ib3	Combined D,A lifetimes	Frequency domain: τ_ϕ, τ_m correlations	20,75
Ib4	Spectral FLIM (sFLIM)	D and A lifetimes as functions of λ_{exc}, λ_{em}	77,79,81
Ic. Donor intensity and intensity ratios			
Ic1	Intensity	$\rho = I/I_o$	
Ic2	On-off ratio	$\rho = \mathrm{OnOff_o}/\mathrm{OnOff}$	Proposed
Ic3	Excited state saturation	$\rho = \zeta/\zeta_o$; $\zeta = \dfrac{\Psi_2/\Psi_1 - I_2/I_1}{I_2/I_1 - 1}$	Proposed
Ic4	Ground state depletion (triplet)	$\theta = \left(\dfrac{1}{\sigma\tau_T\Psi}\right)\left(\dfrac{Q_f}{Q_{isc}}\right)\dfrac{(1-\varphi)(1-\varphi_o)}{\varphi-\varphi_o}$; $\varphi = \dfrac{I_{long}}{I_{short}}$	Proposed
Id. Donor depletion kinetics			
Id1	D pb kinetics (pbFRET)	$\rho = \tau_{pb,o}/\tau_{pb}$	25,26,84,85
Id2	Integrated D pb	$\rho = \zeta/\zeta_o$; $\zeta = I(t=0)/\int_o^\infty I(t)dt$	25,84
Id3	Intersystem crossing	$\rho = \tau_{isc,o}/\tau_{isc}$	Proposed
Ie. Acceptor depletion (adFRET)			
Ie1	Direct A pb (irreversible)	Combination with Ib1–2, Ic1–4, Id1–3, IIa1	26,86,87
Ie2	Photochromic A (pcFRET)	Combinations as in Ie1; example (with Ic1): $\rho = 1 - \dfrac{1 - I_{on}/I_{off}}{\alpha_{on} - \alpha_{off}(I_{on}/I_{off})}$	27,28
Ie3	A saturation (frustrated FRET)	Combinations as in Ie1; example (with Ic1): $\rho = \alpha_{sat}(I_{\alpha_{sat}}/I + \alpha_{sat} - 1)^{-1}$	Proposed
Ie4	Sensitized A pb kinetics (PES)	$\rho = 1 - \dfrac{\sigma_a}{\sigma_d}\left(\dfrac{\tau_{pb,o}}{\tau_{pb}} - 1\right)$	30
II. Emission anisotropy			
IIa. Steady-state anisotropy			
IIa1	Donor anisotropy $\bar{r}$	$\rho = \zeta/\zeta_o$; $\zeta = \left(\dfrac{r_o - \bar{r}}{\bar{r} - r_\infty}\right)$	10,12,88
IIa2	Acceptor anisotropy $\bar{r}$	$\rho = 1 - \dfrac{\sigma_a}{\sigma_d}\left(\dfrac{\bar{r}_o}{\bar{r}} - 1\right)$	Proposed
IIb. Homotransfer, energy migration FRET (emFRET, P-FRET)			
IIb1	Steady-state anisotropy $\bar{r}$	$\bar{r} = \dfrac{r_o(1 - \gamma e^{\gamma^2}\pi^{1/2} erfc[\gamma])}{1 + \tau/\phi}$; $\gamma = \left(\dfrac{Q_o}{1+\tau/\phi}\right)^{1/2}\dfrac{\Gamma_o^3 c}{750}$	1,9,12,31,32,64,88–90
IIb2	Dynamic r (rFLIM, P-FRET)	Functions of r_o, r_∞, ϕ, τ	9,20,31,63,72,83,91

Subscripts refer either to species composition, excitation or photophysical process; a subscript 'o' refers to a reference state of either D (assumed unless otherwise indicated) or A, in which the other component is absent. Superscripts indicate whether emission is measured in the D or A spectral regions and assumes correction for spectral crosstalk (for example, D→A). See equations (1–4) for definition of terms and symbols (σ, Ψ, Q, θ, ρ). I, signal intensity; (Ia3) I_b, bioluminescence signal; (Ic4) I_{long} and I_{short}, signals at end and beginning, respectively, of a given exposure time. In some cases, the need for calibration (scaling) factors is indicated by the symbol '∝'; (Ie2) α_{on}, fractional transition to the FRET-competent photochromic form of the A upon UV irradiation, and α_{off}, fractional transition to the FRET-incompetent photochromic form of the A upon visible irradiation; (Ie3) α_{sat}, degree of light-induced formation of the FRET-incompetent excited state of the A; $I_{\alpha_{sat}}$, D intensity corresponding to α_{sat}; (IIb1) see text for definitions; c in mM units.

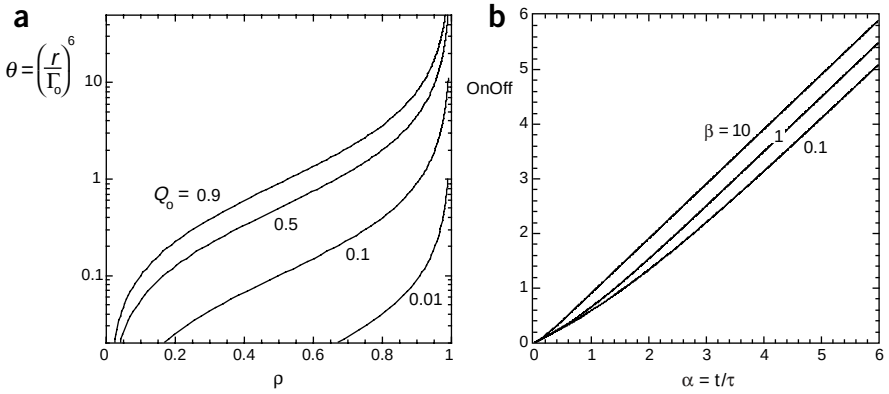

Figure 1 Parametric FRET functions. (**a**) Förster factor θ as a function of a ratio function ρ. The latter involves combinations of parameters or functions equivalent to the ratio of the FRET-quenched and unquenched donor quantum yields, (equation (4) and **Table 1**). Operation in the linear irradiance regime (**Fig. 2**) is assumed. (**b**) FRET technique based on OnOff ratio (equation (4) in **Box 1**), which directly yields the fluorescence lifetime (via α) for any degree of saturation (β).

instead a function of the donor-acceptor separation *r*.

A further issue is the donor-acceptor stoichiometry. In the case of a donor surrounded by *n* equivalent acceptors, the operational R_o^6 is ~*n* times that for the single donor–acceptor pair, and for point-to-plane transfer, the distance dependence varies with the 4th, and not the 6th, power of the separation[22]. In short, the concept of a 'constant' resonance energy transfer (RET) parameter, such as R_o, is not universally applicable.

In our estimation, the relationship of k_t to many of the experimental means for its determination (see **Table 1**) may be expressed more naturally by recourse to alternative formulations, and we propose the one represented in equation (2).

$$\theta \equiv \frac{k_f}{k_t} = \left(\frac{r}{\Gamma_o}\right)^6; \Gamma_o^6 = c_o \kappa^2 J n^{-4}; R_o^6 = Q_o \Gamma_o^6 \qquad (2)$$

$$\theta = Q_o\left(\frac{\rho}{1-\rho}\right); \rho = 1 - E = \frac{Q}{Q_o} \text{ or any other equivalent ratio or function.} \qquad (3)$$

We define the inverse proportionality constant between k_t and k_f as a 'Förster Factor' θ, and equate it to the 6th power of the ratio of the separation distance *r* and a Förster constant Γ_o, in which Q_o is absent. It is important to recognize that the other parameters defining Γ_o may also vary in particular experiments, either by experimental design or nature of particular targets, or from changes in the inherent population distribution of molecular states. In the latter case, appropriate ensemble averaging formalisms must be employed[1,3,11,12–15].

We now extend the formalism further (equation (3)) by relating θ to ρ, a ratio of experimental quantities (**Table 1**) proportional to the donor quantum yields corresponding to the two conditions: donor with acceptor (presence of RET); and donor without acceptor (absence of RET). From equation (3) and **Fig. 1a**, it is seen that a reduction in donor Q_o has two consequences. First, it displaces the transition inflection point, and thus the greatest sensitivity of ρ, from θ = 1 to smaller values (smaller *r*). And second, it restricts the operative dynamic range of the determinations to higher values of ρ. A further consideration, already stated earlier, is that the nonradiative decay pathway and thus Q_o can also change dramatically between alternative molecular states represented in a particular FRET experiment.

A catalog of FRET microscopy methods

In devising methods for exploiting FRET in microscopy, one is faced with two fundamental challenges: first, the formalism must be appropriate for quantifying FRET under conditions of arbitrary, generally unknown, intramolecular and/or intermolecular stoichiometries, distributions and microenvironments of donor and acceptor; second, continuous methods of observation (by FRET) are desirable in most studies of live cells. Numerous other considerations dictate the choice of FRET techniques for imaging purposes and lead us to the classification scheme given in **Table 1**.

We include several new strategies (Ic2–4, Id3, Ie2–3, Ie4, and IIa2) with potential for implementation in fluorescence microscopy. The methods are assigned to two groups (I and II) depending on whether they are based on intensity and kinetic donor-acceptor relationships or on emission anisotropy. In many instances, as in the 'ρ methods' (Ib1–2, Ic1–3, Id1–3, Ie1–4, and IIa1–2), the reference measurement alluded to above (*e.g.*, donor I_o or τ_o) is required. It can be provided either by a separate region or sample, if available, or by recourse to the various acceptor depletion strategies (Ie). The determination of the Förster Factor θ by some other techniques (Ia2–3, IIb1–2) does not require Q_o as a scaling factor.

We stress the desirability of quantitative determinations by supplying equations based on the formalism introduced above. That is, we favor the view that the generation of secondary images representing FRET-related or FRET-derived parameters is the primary goal. The formulas differ as to whether they are restricted to the linear irradiance regime, and apply either to a single donor-acceptor pair or to arbitrary donor-acceptor stoichiometries and thus an ensemble of molecular species. Generalization is possible but beyond the scope of this report; for Monte Carlo simulations of some cases of **Table 1**, see ref. 11.

In the following text, we provide brief explanations of the different entries outlined in **Table 1**. Two points are worth emphasizing at the outset. First, the methods with greatest sensitivity for low transfer efficiencies—in some cases coupled with fast acquisition capability—include Ia2–3, Ib2 and Ie2–4. Second, methods differ with respect to their applicability in point-scanning as opposed to wide-field microscopes.

In well-defined (usually intramolecular) single-donor, single-acceptor systems, fluorescence ratio measurements involving different spectral components (donor and acceptor signals) can be calibrated so as to yield the FRET efficiency. These techniques (Ia1) are difficult to implement because they require acquisition and registration of multiple images,

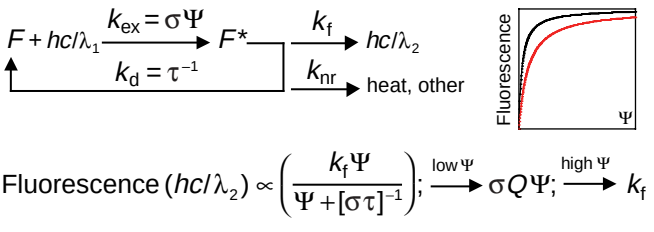

Figure 2 The 'Michaelis-Menten' view of a fluorophore as a photon conversion catalyst or 'enzyme' (see **Box 1**). The two saturation curves depicted differ in στ by a factor of 3 (lower value in red).

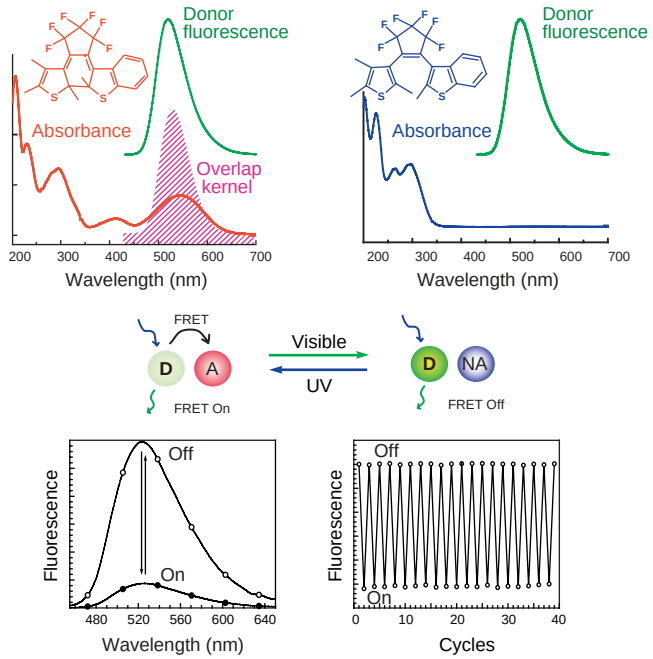

Figure 3 Photochromic FRET (pcFRET). The chemical structures depicted correspond to the photochromic dithienylethene in the colorless open form (right upper) and colored closed form (left upper). The absorption spectrum of the latter overlaps well with the emission spectrum of the donor; the kernel of the overlap integral (striped) corresponds to the lucifer yellow donor selected for a model compound[27]. Ultraviolet light induces the photochromic transition to the closed form (On), and visible (green) light reverses the process to the open form (Off). Bottom: corresponding donor spectra and multiple cycles between the two states of the system. The photophysical scheme is represented in **Figure 5c**.

correction for spectrally overlapping donor and acceptor signals and direct excitation of the acceptor, as well as due consideration of variable donor-acceptor stoichiometries in the equations used to compute ρ and θ. The ratio of the quenched donor and sensitized emission signals (Ia2) is unique in being scaled by the acceptor instead of the donor quantum yield in the calculation of θ. By employing a bioluminescent donor (Ia3)—for example, luciferase as an expressed fusion protein—excitation by light is not required, thereby suppressing autofluorescence background and photobleaching.

The direct determination of fluorescence lifetime (Ib1), either in the time or in the frequency domain, is one of the most direct measures of FRET. It is also relatively insensitive to variations in concentration and optical path length. Selection of a donor with a long lifetime and high transfer efficiency (Ib2), such as lanthanide-chelates, permit sensitive measurements of donor quenching (that is, of very low transfer efficiencies) because the (quenched) donor decay is monitored via the sensitized (shorter-lived) acceptor emission, thereby ensuring a low background. Sample/microenvironmental heterogeneity can be assessed with FRET by exploiting numerous formalisms for time- and frequency-domain measurements (Ib3), particularly if the fluorescent lifetimes can be correlated with continuous emission and/or excitation spectra via multiplexed, transform-encoded acquisition (Ib4).

FRET determinations derived from intensity relationships (Ic1) require an accurate reference for the acceptor-free donor signals and are difficult to achieve in practice except, for example, in combination with acceptor depletion schemes (Ie) or recourse to appropriately fabricated nano-microstructures. The use of 'dark' acceptors falls into this general category.

We introduce here three new approaches (Ic2–4) for the exploitation of intensity measurements by use of the photophysical principles outlined earlier and constituting indirect estimations of the fluorescence lifetime. The first (Ic2) is based on the OnOff function (see **Box 1**, equation (4)). This relationship provides a direct determination of τ for any degree of donor saturation (at saturation, the relationship is linear; see **Fig. 1b**). Implementation should be simple (*e.g.*, using a detector with swinging dual integrated outputs). A second method (Ic3) is based on the displacement to the 'right' of the singlet saturation curve due to the FRET-induced shortening of the fluorescence lifetime (**Fig. 2**). Measurements are performed at two levels of irradiance (denoted by subscripts 1,2 in **Table 1**, Ic3), one of which has to be sufficiently high (that is, above the linear range). The indicated function involving the ratios of irradiances and signals yields στ. The acceptor should have a short lifetime to prevent its saturation via FRET. Distortions of the imaging point-spread-function may arise from donor saturation, particularly when using scanning systems; these effects can either reduce or enhance[23,24] spatial resolution. In wide-field systems, such problems vanish although high-energy sources are required. Finally, in Ic4 we exploit the triplet lifetime τ_T, which can be extended from the microsecond characteristic of oxygen-saturated systems to the millisecond domain (depending on the fluorophore) by oxygen depletion via argon flushing or chemical reductants. Measurements performed after short and long exposure times, defined in relation to τ_T, differ by virtue of depletion of the singlet manifold to an extent reflecting FRET-induced changes in the fluorescence lifetime.

FRET determinations based on donor depletion kinetics are also in widespread use. Donor photobleaching (Id1) occurs with a time constant that is inversely related to the donor quantum yield. Inasmuch as the process generally occurs on a timescale 6–12 orders of magnitude greater than the usual nanosecond range of fluorescence decay, the method is easy to implement. It also circumvents the registration problem of disparate images (assuming no sample movement) and the need for spectral overlap factors (as in Ic1), and does not require a fluorescent acceptor, although the latter must be photostable. Another reason accounting for the popularity of pbFRET is its good performance at low transfer efficiencies. A variant of pbFRET (Id2) introduced at the same time as Id1 (ref. 25) has not been adopted generally, despite its ideal suitability for detection with charge-coupled dipole (CCD) cameras. The underlying principle, first announced by the remarkable spectroscopist, the late Thomas Hirschfeld, is the invariance (quantum yield independence) of the total integrated emission during quantitative photobleaching of a fluorophore. The integrated image serves to normalize a corresponding initial quenched donor image of the same area. A third, new kinetic method (Id3) involves the measurement of the kinetics of ground-state depletion via intersystem crossing to the triplet state of the donor. As in Ic3, one requires conditions favoring the maintenance of a long triplet lifetime.

The methods we have combined under the designation 'acceptor depletion' FRET (adFRET; Ie) are of fundamental importance because they permit the generation '*in situ*,' that is, at every sample position, of the reference state required for many of the other techniques. Note that this category corresponds to 'Γ_o (or R_o) engineering' in the sense that one perturbs the system by altering the value of J (see equation (1)).

In 1995, we implemented irreversible acceptor photobleaching (Ie1) upon noting the difficulty of performing donor pbFRET (Id1) with the very good FRET donor-acceptor pair of cyanine dyes Cy3–Cy5 (ref. 26). Cy3 is highly photostable (the newer version Cy3b even more so), whereas Cy5 photobleaches readily; it became apparent that

photobleaching the latter provided 'before' and 'after' images from which the FRET efficiency could be readily determined. This technique is used extensively due to its many virtues: (i) it is simple and rapid; (ii) only donor images are required, avoiding registration problems; (iii) there is automatic correction for pixel-by-pixel variations in the reference donor quantum yield (lifetime); (iv) it is very effective for high-transfer efficiencies ('disappearing' donor; see Figures 2 and 3 in ref. 26); (v) it works well with 'dirty,' that is, relatively impure acceptors; and (vi) it can be combined with Id1,2 (ref. 26).

Photochromic FRET (pcFRET; Ie2) is the reversible equivalent of Ie1 and thus offers the prospect of continuous measurements with cellular samples. A photochromic acceptor is cycled repeatedly between FRET 'competent (on)' and FRET 'incompetent (off)' states by alternative exposures to visible and UV light[27,28] (**Fig. 3**). Besides being reversible, pcFRET is superior to Ie1 in having a high quantum yield for photoconversion. That is, few absorbed photons are required to induce the interconversions between states, in contrast to ~10^{4-6} photons for irreversible photobleaching. We are adapting pcFRET for microscopy by optimized chemical design of the photochromic probes and incorporation of modulated light sources and detectors to permit very sensitive detection, especially of low FRET efficiencies. In addition, we have devised a scheme for applying the pcFRET concept in determinations of reaction kinetics (pcRelKin, patent applied for by the authors). This relaxation technique is potentially suited for very small volumes and high speed.

Two new adFRET techniques are proposed here. In the first (Ie3), the acceptor is driven into saturation so as to 'frustrate' FRET[23,29], and thereby restore the donor emission to its unquenched level. The use of modulated light sources (of which two are required) and phase-sensitive detection (with a lock-in amplifier) should provide a very sensitive measurement, particularly in laser spot scanning systems. A photostable long-lived acceptor is required.

Another new and intriguing FRET method (Ie4), to our knowledge not yet applied in microscopy, was designed to detect extremely low FRET efficiencies in solution (the author claimed the potential for detecting an E of 10^{-4} over a distance of 20 nm[30]). This technique is based on the measurement of the photobleaching kinetics of a photolabile acceptor excited by a donor via FRET. The low background and high sensitivity are achieved by exciting the donor, preferably a fluorophore with a large Stokes shift, at a wavelength of minimal absorption by the acceptor.

Emission anisotropy, a dimensionless quantity defined in terms of the two polarized emission signals arising from polarized excitation, provides a steady-state ($\bar{r}$) or time-dependent measure of rotational diffusion and is thus sensitive to size, shape, association and motion. The parametric descriptors are the fluorescence lifetime, the rotational correlation time(s) ϕ, and the initial (r_o) and final (r_∞, limiting) anisotropies dictated by the intrinsic transition moments and molecular asymmetry, and the environmental anisotropy, respectively. The determination is based on signal ratios and thus shares with the lifetime a relative insensitivity to optical thickness, light intensity and concentration. We can identify at least two FRET methods based on fluorescence anisotropy. By virtue of the relationship between the rotational diffusion parameters, the donor $\bar{r}$ is a function of the ratio τ/ϕ[31]; thus, a change in the lifetime will be reflected in $\bar{r}$ (IIa1). We propose a second technique (IIa2) involving the selection of an excitation wavelength capable of exciting both the donor and acceptor and thus leading to both direct and indirect (FRET-sensitized) emissions of the latter. The sensitized component is virtually depolarized and thus the mean $\bar{r}$ for the interrogated molecular population provides a measure of FRET. An acceptor with a large Stokes shift is required. There exists an obvious relationship to method Ie4.

The emission anisotropy is also the basis of FRET determinations

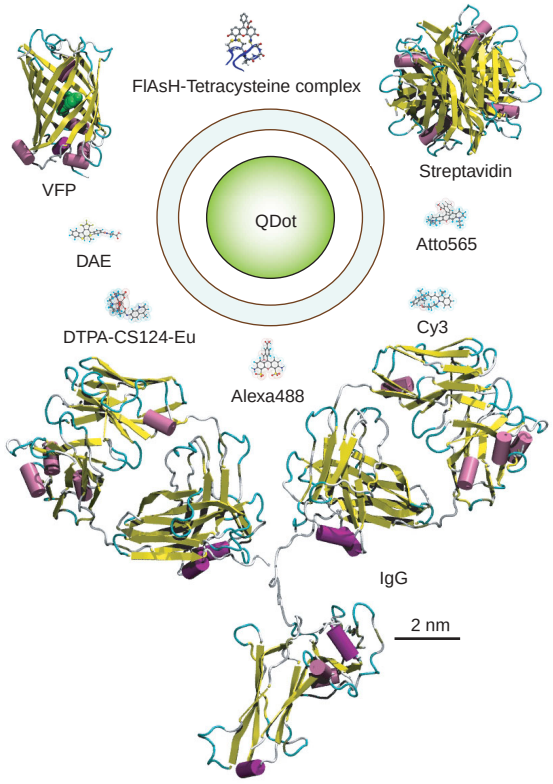

Figure 4 Comparative sizes of common fluorophores and protein carriers used in FRET imaging. Small molecules are represented with Chem3D Ultra (CambridgeSoft). Molecular structures of the small dyes were obtained from available crystallographic data or by minimization using molecular modeling (MM2). DAE, DTPA-CS-EU and ATTO correspond to the dithienylethene depicted in **Figure 3**, the complex of DTPA-carbostyryl 124 with europium[70] and a representative of the Atto dye family (Atto-Tec), respectively. The FlAsH compound is shown as a complex with a 32 amino acid peptide containing a CCGPCC target[39]. The scale bar applies to all molecules. Information required for the depiction of the quantum dot (core, shell, and cap of Qdot 585 Streptavidin Conjugate) was kindly provided by Marcel Bruchez of Quantum Dot. We are greatly indebted to Reinhard Klement for the protein and peptide representations.

measuring the distribution of excited-state energy between identical molecules in close proximity, a process termed homotransfer (or energy migration) RET. EmFRET (our notation[31]) constitutes a sensitive measure of bulk concentration (in the 0.1–10 mM range) and/or of molecular association and clustering in solution (three dimensions) or in planar membranes (two dimensions). One can readily distinguish, for example, between dimerizing and monomeric VFPs with this technique[32]. The depolarization is due to the loss of orientational correlation between excitation and emission but leaving the ensemble lifetime and spectra unaltered. We have demonstrated emFRET in bacteria expressing VFPs[20,31] and in signal transduction mediated by growth factors and their cognate receptor tyrosine kinases fused with VFPs[32] (for other applications, see references in **Table 1;** IIb1,2). One great advantage of emFRET is the requirement for the expression *in vivo* of only a single VFP or other expression probe, as opposed to the requirement for two distinct donor and acceptor molecules in heterotransfer RET. In biotechnological applications, the ability to determine concentrations at the microscopic scale using a dimensionless parameter should be of considerable interest.

In summary, both static (IIb1) and dynamic (IIb2) anisotropies can

Box 1 Photophysical primer

One can regard a given fluorophore as a photophysical catalyst that in a real functional sense shares many attributes of a protein catalyst (an enzyme). That is, the steady-state formalism of the familiar Michaelis-Menten kinetics applies directly to the transformation by a fluorophore F of its 'substrate'—a photon (of wavelength λ_1 and energy hc/λ_1; h, Planck's constant; and c, velocity of light)—that 'binds' (is absorbed) into a 'product'—a photon at longer wavelength λ_2 (and of lesser energy hc/λ_2) with an efficiency dictated by alternative nonradiative pathways (**Fig. 2**).

At low 'substrate concentration,' the rate of photon emission is linearly dependent on light intensity, or more precisely, photon flux Ψ (photons s^{-1} cm^{-2}) = 5×10^{15} irradiance (W cm^{-2}) × wavelength (nm). The photonic 'K_M', the value of Ψ yielding half the maximal fluorescence signal, is given by $[\sigma\tau]^{-1}$, where σ is the absorption cross-section (a measure of photon capture probability, a quantity proportional to the decadic molar absorption coefficient ε; $\sigma = 3.8 \times 10^{-21}\varepsilon$), and τ is the first excited singlet state ($S_1 = F^*$) lifetime; $\tau = k_d^{-1} = [k_f + k_{nr}]^{-1}$; k_f and k_{nr} are the radiative and nonradiative deactivation rate constants, respectively, excluding for the moment other competing processes described below. The initial slope (emission versus excitation photon flux), equivalent to the enzymatic k_{cat}/K_M, is given by σQ; the fluorescence quantum yield (Q) is defined as the ratio of emitted to absorbed photons or by the equivalent expression $k_f/k_d = k_f\tau$. The process saturates at high 'substrate concentration' (irradiance; **Fig. 2**) because the fluorophore is maintained in the excited singlet state (assuming the absence of a finite triplet steady-state population), thus yielding a maximal 'turnover' rate equal to k_f. This maximal rate of fluorescence emission, given by the reciprocal of the radiative lifetime, is independent of Q and of the excitation light intensity and stability, implying that the most sensitive, quantitative, rapid and possibly simplest determination of molecular number, local density or concentration may often be achieved by operating at saturation instead of in the low, linear, range universally espoused for quantitative biological microscopy.

The total photon yield/fluorophore/pulse (PY) for a rectangular excitation pulse of length $t = \alpha\tau$, and photon flux $\psi = \beta/(\sigma\tau)$ is given by equation (4), in which PY_{on} and PY_{off} are the integrated photon emissions during the light (irradiation) and dark (post-irradiation decay) phases, respectively. For $\beta >> 1$ (the saturation condition): $PY \rightarrow Q(1+\alpha)$ and the ratio function OnOff $\rightarrow\alpha$. If α is also >>1 (that is, $t >> \tau$) $PY \rightarrow Q\alpha \equiv k_f t$, confirming the result derived above from the steady-state solution in **Figure 2**.

$$PY = \frac{Q\beta\left[\alpha + (1 + \alpha - e^{-\alpha(1+\beta)})\beta\right]}{(1+\beta)^2} = PY_{on} + PY_{off}$$

$$PY_{on} = \frac{Q\beta\left[e^{-\alpha(1+\beta)} - 1 + \alpha(1+\beta)\right]}{(1+\beta)^2};\ PY_{off} = \frac{Q\beta(1 - e^{-\alpha(1+\beta)})}{1+\beta}$$

$$OnOff = \frac{PY_{on}}{PY_{off}} = \frac{\alpha}{1 - e^{-\alpha(1+\beta)}} - \frac{1}{1+\beta} \quad (4)$$

Saturation can be achieved to any desired degree by selection of light pulses of a given repetition rate, duty cycle and duration. These parameters are generally selected so as to reduce background, triplet state buildup, photodestruction and generation of potentially cytotoxic photoproducts (see valuable discussions in refs. 23,92). One can minimize the latter two reactions by limiting the photon dose (irradiance × exposure time ∝ $\alpha\beta$).

According to equation (4), a single fluorescein-like molecule ($\varepsilon = 10^5$ M^{-1} cm^{-1}, $\tau = 4$ ns, $Q = 0.4$) exposed to an 8-ns pulse of 0.2 nJ at 488 nm focused to an area of 1 μm^2 ($\alpha = 2$, $\beta = 9.3$) will on average emit 0.69 photons in the light phase and 0.36 photons in the dark phase; the OnOff ratio, 1.9, is very close to α, in accordance with the limiting cases given for equation (4) (see also **Fig. 1b**). The ratio of PY to a given irradiation 'dose' ($\alpha\beta = 18.5$ photons in the above example) constitutes a measure of 'photon conversion efficiency' and thus of signal-to-background contrast. In the event of significant contributions from scattering and short-lived luminescent components, one may wish to gate detection during the pulsed excitation cycle, thereby restricting the signal to PY_{off}.

Photobleaching limits the number of cycles (photon 'turnovers') to $\sim\tau_{pb}/\tau$, in which τ_{pb} is the reciprocal photobleaching rate (**Fig. 5**). A typical value is $\sim 10^5$ cycles (fluorescein), implying that $\sim 10^2$ repetitions would be possible for single determinations based on 10^3 excitation pulses. On the other hand, photobleaching can also be exploited to obtain information, as in determinations of FRET (pbFRET, Id1 and Id2, **Table 1**) and of translational diffusion (FRAP, FLIP[86] and FLAP[93]).

To explore quantitatively the region of saturation (that is, depletion of the ground state), we are obliged to expand the formalism to account for transitions to and from the triplet state, RET between donor and acceptor fluorophores and photobleaching (**Fig. 5a**). The corresponding rate equations for a complete kinetic scheme are first-order except for the virtual second-order RET reaction involving donor* (D*) and acceptor (A) in the forward and acceptor* (A*) and donor (D) in the reverse direction. We circumvent this difficulty by representing the system in terms of transitions between donor-acceptor pairs in the different electronic states (**Fig. 5b**), thereby obtaining analytical expressions that permit the exploration of arbitrary degrees of saturation of both donor and acceptor (see also ref. 29).

report changes in conformation, association and FRET. These techniques are being implemented in numerous microscope systems, most recently in a confocal laser scanning microscope adapted with dual channel polarization detection[32].

Probes and strategies

Solely from the standpoint of stability and brilliance of a fluorophore, one can define a 'figure of merit,' such as the product $\sigma k_f Q_f Q_{pb}^{-1} Q_{isc}^{-1} = \sigma Q_f^2 [\tau Q_{bl} Q_{isc}]^{-1}$. The commercial sources stress σ and Q_f, as exemplified by the cyanines (Amersham Biosciences), Alexa (Molecular Probes) and the long-wavelength Atto (Atto-Tec) series of dyes. However, other considerations apply depending on the FRET method adopted for use (**Table 1**). For example, in donor pbFRET (Id1,Id2) excessive photostability is undesirable, whereas for the methods based on ground state depletion by intersystem crossing (Ic4,Id3), Q_{isc} must be finite. It may also be necessary to tailor the donor lifetime in relation to the dynamics of the particular process under investigation, and although in most cases a large Stokes shift is desirable so as to minimize crossover of the donor fluorescence into the acceptor emission band, a small Stokes shift is required for homotransfer FRET (IIb). Another consideration is the

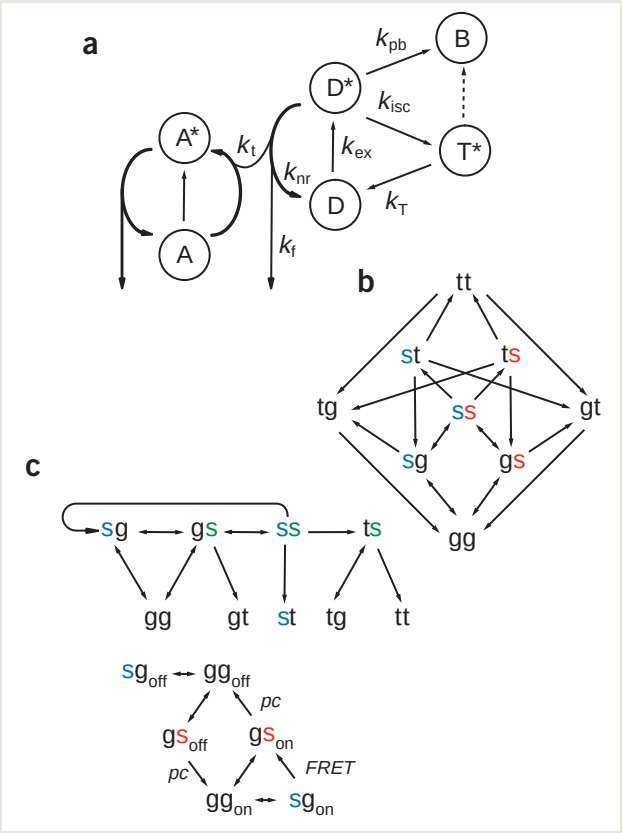

Figure 5 Photophysical cycles including triplet state, FRET, and photobleaching. (**a**) Coupling of donor and acceptor. For simplicity, only the triplet and bleached states of the donor, D, are indicated; the rate constants for the acceptor, A, are also omitted. Definition of rate constants: $k_{ex} = \sigma\psi$; k_{isc}, intersystem crossing (D*→T* transfer); $k_T = \tau_T^{-1}$, triplet decay; k_t, FRET (D*→A* transfer); k_{pb}, photobleaching (can also involve T*). For the usual nanosecond fluorophores lacking heavy atom substituents, k_{isc}, k_{pb}, k_T are << k_f, k_{nr}. (**b**) Photophysical state diagram based on twofold D-A combinations. Each pair consists of a D (left) and A (right) in any of four states: ground (g), excited singlet (blue, red and green s), excited triplet (t) and bleached (not shown). All transitions except FRET are depicted. (**c**) Cycle involving acceptor states excited exclusively via FRET (top), shown as the double-headed arrow (forward and reverse transfer) between sg and gs, and (bottom) of FRET-linked photochromic cycle depicted in **Figure 3**. Analytical, albeit complex, solutions for the corresponding time-dependent and stationary states for the schemes of **b** and **c** have been obtained with Mathematica, including arbitrary degrees of saturation of the D and/or A and explicit consideration of the FRET-excited acceptor species, thereby permitting the calculation of the time course of acceptor anisotropy.

means by which the probe is linked to the target molecule. One might wish to constrain the κ^2 conundrum by introducing flexibility, yet in anisotropy-based FRET determinations (IIb) rigidity is preferable, such as with the bisarsenylated fluorescein (FlAsH; see below) and bifunctional[33] probes. Similar considerations apply to the acceptor, with which the spectral overlap and absorptivity of the acceptor dictate the sensitivity to distance modifications in a given range. However, in cases where the range of lower donor-acceptor separations is of interest, a smaller Γ_o (that is, J) may be required so as to define a 'working region' optimized around the value $\theta = 1$; see **Figure 1a**.

Current expression probes for determining molecular concentration, distribution and 'age' *in vivo* are primarily based on protein fusions with VFPs of jellyfish or coral origin (reviewed in refs. 4,5,7); other molecular FRET-active VFP derivatives are also available[34,35]. Recent developments in the VFP field, all of which are relevant for FRET, include mutants with increased spectral range, photoconversion capabilities, improved photostability and brightness, faster maturation rate and suppressed tendency to oligomerize. The advent of a photoactivatable VFP[5] is of particular significance. Localized application of blue light to cells—two-photon activation may also be possible—permits the activation of a fluorescence signal at an arbitrary location and time, an invaluable feature for studies of protein translocation and association.

Many new reporters based on donor-acceptor FRET pairs linked by a moiety that undergoes a conformational change upon binding or modification events have been devised[4,5,7,34]. The resulting perturbation of the FRET signal serves as a monitor of the underlying time-dependent process such as protein (de)phosphorylation or ion binding in the specific cellular compartment. A recent FRET-like addition to the VFP toolbox is bimolecular fluorescence complementation (BiFC), conceived as a means for assessing multiple protein-protein interactions *in vivo* with very low background[36]. Nonfluorescent fragments of spectrally distinct VFPs are fused to different proteins of interest. If the latter associate in the cell, the coupled VFP fragments associate and exhibit fluorescence after a maturation period. This technique joins related complementation strategies for studying protein-protein interactions, such as the protein fragment complementation assay (PCA), and the generation of fluorescence or bioluminescence by intein-mediated protein splicing of fragmented VFP or luciferase, respectively[37]. All of these approaches have potential for FRET-based enhancements or implementations, such as with bioluminescence resonance energy transfer in the case of luciferase (**Table 1;** Ia3). In all the VFP-based techniques, two fundamental problems must be faced, namely the possible functional consequences of overexpression and the need to distinguish between VFP-fused proteins delivered to their natural cellular compartment from nascent, reclaimed and degraded molecules elsewhere in the cell. Total internal reflection microscopy[10,38] and other superresolution techniques (S. Hell, this issue) should be of great utility in this respect.

New strategies and dyes with improved properties will expand the capabilities for *in vivo* FRET applications. The combination of exogenous probes and the expression of small peptide targets offer the advantage of greatly reduced size compared to VFPs (**Fig. 4**) and the versatility offered by the ligand in terms of lifetime, large Stokes shift or other property. One such system is based on specific hexapeptide sequences containing four cysteines and introduced into a target protein of interest. Application of an exogenous, membrane permeable, nonfluorescent probe, such as FlAsH or resorufin (ReAsH) derivatives, leads to binding to the tag and the generation of a specific fluorescent signal[39]. We have devoted great effort to developing functional derivatives of these very promising reagents but consider that additional chemical modifications are required to reduce the background in cellular applications (see also ref. 40). Other potential routes might exploit protein fusions with an anti-fluorophore single-chain antibody fragment[41], novel protein scaffolds ('affibodies'[42]), and a newly reported strategy for introducing unnatural amino acid side chains into proteins[43]. The latter may offer targets for a range of chemical and spectroscopic probes, including those suitable for FRET.

Bioconjugated semiconductor quantum dots offer an alternative to organic molecules as fluorescence probes. Quantum dots are finding widespread application as labeling reagents for cells and macromolecules because of their unique properties and commercial availability[44,45]. Appropriately designed quantum dots are very photostable and

nontoxic, can be excited with one or more[46] photons over a wide spectral range, yet emit in a narrow and programmable spectral range. Quantum dots are typically capped with a polymer bearing specific binding moieties, such as streptavidin, protein G, biotin or conjugatable chemical groups (available through such companies as Quantum Dot or Evident Technologies). We have demonstrated the utility of quantum dots as FRET donors in aqueous systems, a further property of these extraordinary materials that will undoubtedly lead to many applications. An important issue relates to size—whether 'the tail wags the dog'—such that a quantum dot–linked probe would interfere or even abrogate the process under study. A graphical representation designed to convey the relative sizes of various common fluorophores and protein probes compared with a quantum dot is provided in **Figure 4**. One is struck by the extent of the IgG molecule, particularly considering the multistep signal amplification schemes in common use.

Several other probes and small particles are of relevance to FRET applications: (i) transfer probes consisting of diffusible, tyramide-linked fluorophores or haptens rendered reactive by peroxidase fused to a target protein or antibody (*e.g.*, the tyramide signal amplification system offered by Molecular Probes); (ii) photoreactive probes that phototransfer from a given protein to an (unknown) partner, for example, in a photocrosslinking reaction[47] mediated by the PES (photochemical enhancement of sensitivity)-FRET mechanism (**Table 1**, Ie4); (iii) microspheres, nanocrystals and phosphors that can be evaluated on and in cells by virtue of attached ligands, morphology, spectroscopy and/or localization and functional effects; (iv) the photochromic probes described above (**Table 1**, Ie2; **Fig. 3**); (v) cascade FRET[23,48] and photoinducible intramolecular charge transfer[49] probes; and (vi) many versions of 'dark' acceptors with very high σ and consequently large Γ_o values. An important issue with these and other nonexpression probes is the method of introduction into the molecule and/or the cell.

Perspectives

Single-molecule spectroscopy based on fluorescence has developed since the pioneering work Thomas Hirshfeld in the 1970s and in many instances is implemented with imaging technology. FRET is an essential tool[10,50,51] in this field, and should augment the high-resolution techniques recently exemplified in very elegant studies of myosin V dynamics[33,52]. Attempts to confine single-molecule measurements to nanocavities have succeeded in extending the operational range of fluorescence correlation spectroscopy (FCS) to the heretofore inaccessible micromolar range[53] (W. Webb, this issue). Such cellular structures may be suitable for new FRET implementations in FCS[54] and image correlation spectroscopy[55], as well as two-dimensional FCS spectroscopy based on modulated excitation[56], perhaps exploiting the dramatic enhancements of excitation energy transfer achieved in Fabry–Perot microresonators[57]. Scanning near-field optical microscopy (SNOM) provides many interesting imaging possibilities (A. Lewis, this issue), including a donor-coated 'self-sharpening' scanning tip limiting the extent of the corresponding acceptor array to tens of molecules[58]. The same laboratory has recently reported the integration of quantum dots as FRET-SNOM sources with the prospect of single molecule resolution[59], and a coherent mode of operation extending the transfer distance to 20 nm with implications for quantum computing[60]. In the case of cellular imaging based on FRET, one can predict great utility for highly integrated nanochambers[61] and cellular microarrays[62].

We anticipate that many of the newer approaches for FRET microscopy outlined in **Table 1** will come to fruition, hopefully integrated into the full array of emerging multidimensional microscopy techniques, particularly those adapted for optical sectioning. A concrete application representing a core research activity of our groups[32] is the elucidation of ligand-mediated modulation of receptor-receptor distributions and dynamics[63,64,65] on cell surfaces. The ongoing challenge is to expand further the algorithmic repertoire for dissecting such complex molecular systems into their component contributions. It is axiomatic that the full panoply of temporal, spatial and spectral resolution will be required.

ACKNOWLEDGMENTS

E.A.J.-E. is indebted to the Agencia Nacional de Promoción de la Ciencia y Tecnología (ANPCyT), Fundación Antorchas, Consejo Nacional de Investigaciones Científicas y Técnicas (CONICET), Secretaría de Ciencia, Tecnología e Innovación Productiva (SECyT) and the Universidad de Buenos Aires (UBA) for financial support. T.M.J. was supported by the Max Planck Society, European Union FP5 Projects QLG1-2000-01260 and QLG2-CT-2001-02278, and the Center of the Molecular Physiology of the Brain funded by the German Research Council (DFG). The authors were the recipients of a joint grant from the Volkswagen Foundation for their work on photochromic compounds and acknowledge the contribution of graduate student Luciana Giordano to the research depicted in Figure 4, as well as the efforts of many colleagues over the years in the general area represented by this review. They are also indebted professionally and personally for the inspiration offered by the late Gregorio Weber, the acknowledged father of fluorescence in biology. We thank Rainer Heintzmann, Pedro Aramendía, Carla Spagnuolo and Vinod Subramaniam for critical reading of the manuscript.

COMPETING INTEREST STATEMENT

The authors declare that they have no competing financial interests.

Published online at http://www.nature.com/naturebiotechnology/

1. Wieb Van Der Meer, B., Coker, G. III & Simon Chen, S.-Y. *Resonance Energy Transfer: Theory and Data* (VCH, New York, 1994).
2. Hink, M.A., Bisselin, T. & Visser, A.J. Imaging protein–protein interactions in living cells. *Plant Mol. Biol.* **50**, 871–883 (2002).
3. Hoppe, A., Christensen, K. & Swanson, J.A. Fluorescence resonance energy transfer-based stoichiometry in living cells. *Biophys. J.* **83**, 3652–3664 (2002).
4. Zhang, J., Campbell, R.E., Ting, A.Y. & Tsien, R.Y. Creating new fluorescent probes for cell biology. *Nat. Rev. Mol. Cell Biol.* **3**, 906–918 (2002).
5. Lippincott-Schwartz, J. & Patterson, G.H. Development and use of fluorescent protein markers in living cells. *Science* **300**, 87–91 (2003).
6. Meyer, T. & Teruel, M.N. Fluorescence imaging of signaling networks. *Trends Cell Biol.* **13**, 101–106 (2003).
7. Miyawaki, A. Visualization of the spatial and temporal dynamics of intracellular signaling. *Dev. Cell* **4**, 295–305 (2003).
8. Sekar, R.B. & Periasamy, A. Fluorescence resonance energy transfer (FRET) microscopy imaging of live cell protein localizations. *J. Cell Biol.* **160**, 629–633 (2003).
9. Marriott, G. & Parker, I. (eds.). *Biophotonics, Part A. Methods in Enzymology*, vol. 360 (Academic Press, San Diego, CA, 2003).
10. Marriott, G. & Parker, I. (eds.). *Biophotonics, Part B. Methods in Enzymology*, vol. 361 (Academic Press, San Diego, CA, 2003).
11. Berney, C. & Danuser, G. FRET or no FRET: a quantitative comparison. *Biophys. J.* **84**, 3992–4010 (2003).
12. Andrews, D.L. & Demidov, A.A. (eds.). *Resonance Energy Transfer* (John Wiley & Sons, Chicester, UK, 1999).
13. Valeur, B. *Molecular Fluorescence: Principles and Applications* (Wiley-VCH, Weinheim, 2002).
14. Clegg, R.M. Fluorescence resonance energy transfer and nucleic acids. *Methods Enzymol.* **211**, 353–388 (1992).
15. Clegg, R.M. Fluorescence resonance energy transfer (FRET) in *Fluorescence Imaging Spectroscopy and Microscopy* (eds. Wang, X.F. & Herman, B.) 179–252 (John Wiley & Sons, New York, 1996).
16. Edelhoch, H., Brand, L. & Wilchek, M. Fluorescence studies with tryptophyl peptides. *Isr. J. Chem.* **1**, 216–217 (1963).
17. Clegg, R.M., Holub, O. & Gohlke, C. Fluorescence lifetime-resolved imaging: measuring lifetimes in an image. *Methods Enzymol.* **360**, 509–542 (2003).
18. Förster, T. Delocalized excitation and excitation transer in *Modern Quantum Chemistry Part III: Action of Light and Organic Crystals* (ed. Sinanoglu, O.) 93–137 (Academic Press, New York, 1965).
19. Volkmer, A., Subramaniam, V., Birch, D.J. & Jovin, T.M. One- and two-photon excited fluorescence lifetimes and anisotropy decays of green fluorescent proteins. *Biophys. J.* **78**, 1589–1598 (2000).
20. Subramaniam, V., Hanley, Q.S., Clayton, A.H.A. & Jovin, T.M. Photophysics of green and red fluorescent proteins: implications for quantitative microscopy. *Methods Enzymol.* **360**, 178–201 (2003).
21. Patterson, G.H., Piston, D.W. & Barisas, B.G. Förster distances between green fluorescent protein pairs. *Anal. Biochem.* **284**, 438–440 (2000).
22. Kuhn, H. in *Physical Methods of Chemistry,* vol. 1 (eds. Weissberger, A. & Rossiter, B.) 579–650 (John Wiley & Sons, New York, 1972).
23. Schönle, A., Hänninen, P.E. & Hell, S.W. Nonlinear fluorescence through intermolecular

energy transfer and resolution increase in fluorescence microscopy. *Ann. Phys. (Leipzig)* **8**, 115–133 (1999).
24. Heintzmann, R., Jovin, T.M. & Cremer, C. Saturated patterned excitation microscopy (SPEM)—a novel concept for optical resolution improvement. *J. Opt. Soc. Am. A* **19**, 1599–1609 (2002).
25. Jovin, T.M. & Arndt-Jovin, D.J. FRET microscopy: digital imaging of fluorescence resonance energy transfer. in *Cell Structure and Function by Microspectrofluometry* (eds. Kohen, E., Hirschberg, J.G. & Ploem, J.S.) 99–117 (Academic Press, London, 1989).
26. Bastiaens, P.I.H. & Jovin, T.M. Fluorescence resonance energy transfer microscopy in *Cell Biology: A Laboratory Handbook,* vol. 3, edn. 2 (ed. Celis, J.E.) 136–146 (Academic Press, New York, 1998).
27. Giordano, L., Jovin, T.M., Irie, M. & Jares-Erijman, E.A. Diheteroarylethenes as thermally stable photoswitchable acceptors in photochromic fluorescence resonance energy transfer (pcFRET). *J. Am. Chem. Soc.* **124**, 7481–7489 (2002).
28. Song, L., Jares-Erijman, E.A. & Jovin, T.M. A photochromic acceptor as a reversible light-driven switch in fluorescence resonance energy transfer (FRET). *J. Photochem. Photobiol. A* **150**, 177–185 (2002).
29. Hänninen, P.E., Lehtelä, L. & Hell, S.W. Two- and multiphoton excitation of conjugate-dyes using a continuous wave laser. *Optics Comm.* **130**, 29–33 (1996).
30. Mekler, V.M. A photochemical technique to enhance sensitivity of detection of fluorescence resonance energy transfer. *Photochem. Photobiol.* **39**, 615–620 (1994).
31. Clayton, A.H.A., Hanley, Q.S., Arndt-Jovin, D.J., Subramaniam, V. & Jovin, T.M. Dynamic fluorescence anisotropy imaging microscopy in the frequency domain (rFLIM). *Biophys. J.* **83**, 1631–1649 (2002).
32. Lidke, D.S. *et al.* Imaging molecular interactions in cells by dynamic and static fluorescence anisotropy (rFLIM and emFRET). *Biochem. Soc. Trans.*, **31**, 1020–1027 (2003).
33. Forkey, J.N., Quinlan, M.E., Shaw, M.A., Corrie, J.E.T. & Goldman, Y.E. Three-dimensional structural dynamics of myosin V by single-molecule fluorescence polarization. *Nature* **422**, 399–404 (2003).
34. Sato, M., Ozawa, T., Inukai, K., Asano, T. & Umezawa, Y. Fluorescent indicators for imaging protein phosphorylation in single living cells. *Nat. Biotechnol.* **20**, 287–294 (2002).
35. Zacharias, D.A., Violin, J.D., Newton, A.C. & Tsien, R.Y. Partitioning of lipid-modified monomeric GFPs into membrane microdomains of live cells. *Science* **296**, 913–916 (2002).
36. Hu, C.D. & Kerppola, T.K. Simultaneous visualization of multiple protein interactions in living cells using multicolor fluorescence complementation analysis. *Nat. Biotechnol.* **21**, 539–545 (2003).
37. Ozawa, T. & Umezawa, Y. Peptide assemblies in living cells. Methods for detecting protein–protein interactions. *Supramol. Chem.* **14**, 271–280 (2002).
38. Riven, I., Kalmanzon, E., Segev, L. & Reuveny, E. Conformational rearrangements associated with the gating of the G protein-coupled potassium channel revealed. *Neuron* **38**, 225–235 (2003).
39. Gaietta, G. *et al.* Multicolor and electron microscopic imaging of connexin trafficking. *Science* **296**, 503–507 (2002).
40. Falk, M.M. Genetic tags for labelling live cells: gap junctions and beyond. *Trends Cell Biol.* **12**, 399–404 (2002).
41. Farinas, J. & Verkman, A.S. Receptor-mediated targeting of fluorescent probes in living cells. *J. Biol. Chem.* **274**, 7603–7606 (1999).
42. Karlström, A. & Nygren, P.-A. Dual labeling of a binding protein allows for specific fluorescence detection of native protein. *Anal. Biochem.* **295**, 22–30 (2001).
43. Chin, J.W. *et al.* An expanded eukaryotic genetic code. *Science* **301**, 964–967 (2003).
44. Wu, X.Y. *et al.* Immunofluorescent labeling of cancer marker Her2 and other cellular targets with semiconductor quantum dots. *Nat. Biotechnol.* **21**, 41–46 (2003).
45. Jaiswal, J.K., Mattoussi, H., Mauro, J.M. & Simon, S.M. Long-term multiple color imaging of live cells using quantum dot bioconjugates. *Nat. Biotechnol.* **21**, 47–51 (2003).
46. Larson, D.R. *et al.* Water-soluble quantum dots for multiphoton fluorescence imaging *in vivo*. *Science* **300**, 1434–1436 (2003).
47. Fancy, D.A. *et al.* Scope, limitations and mechanistic aspects of the photo-induced cross-linking of proteins by water-soluble metal complexes. *Chem. Biol.* **7**, 697–708 (2000).
48. Haustein, E., Jahnz, M. & Schwille, P. Triple FRET: a tool for studying long-range molecular interactions. *Chemphyschem* **4**, 745–748 (2003).
49. Sauer, M. Single-molecule-sensitive fluorescent sensors based on photoinduced intramolecular charge transfer. *Angew. Chem. Int. Ed. Engl.* **42**, 1790–1793 (2003).
50. Michalet, X. & Weiss, S. Single-molecule spectroscopy and microscopy. *C.R. Phys.* **3**, 619–644 (2002).
51. Ishijima, A. & Yanagida, T. Single molecule nanobioscience. *Trends Biochem. Sci.* **26**, 438–444 (2001).
52. Yildiz, A. *et al.* Myosin V walks hand-over-hand: single fluorophore imaging with 1.5-nm localization. *Science* **300**, 2061–2065 (2003).
53. Levene, M.J. *et al.* Zero-mode waveguides for single-molecule analysis at high concentrations. *Science* **299**, 682–686 (2003).
54. Widengren, J., Schweinberger, E., Berger, S. & Seidel, C.A.M. Two new concepts to measure fluorescence resonance energy transfer via fluorescence correlation spectroscopy: theory and experimental realizations. *J. Phys. Chem. A* **105**, 6851–6866 (2001).
55. Rocheleau, J.V., Wiseman, P.W. & Petersen, N.O. Isolation of bright aggregate fluctuations in a multipopulation image correlation spectroscopy system using intensity subtraction. *Biophys. J.* **84**, 4011–4022 (2003).
56. He, Y., Wang, G., Cox, J. & Geng, L. Two-dimensional fluorescence correlation spectroscopy with modulated excitation. *Anal. Chem.* **73**, 2302–2309 (2001).
57. Hopmeier, M., Guss, W., Deussen, M., Gobel, E.O. & Mahrt, R.F. Control of the energy transfer with the optical microcavity. *Int. J. Mod. Phys. B* **15**, 3704–3708 (2001).
58. Shubeita, G.T., Sekatskii, S.K., Dietler, G. & Letokhov, V.S. Local fluorescent probes for the fluorescence resonance energy transfer scanning near-field optical microscopy. *Appl. Phys. Lett.* **80**, 2625–2627 (2002).
59. Shubeita, G.T. *et al.* Scanning near-field optical microscopy using semiconductor nanocrystals as a local fluorescence and fluorescence resonance energy transfer source. *J. Microsc.* **210**, 274–278 (2003).
60. Sekatskii, S.K., Chergui, M. & Dietler, G. Coherent fluorescence resonance energy transfer: construction of nonlocal multiparticle entangled states and quantum computing. *Europhys. Lett.* **63**, 21–27 (2003).
61. Guijt-van Duijn, R.A. *et al.* Miniaturized analytical assays in biotechnology. *Biotechnol. Adv.* **21**, 431–444 (2003).
62. Ziauddin, J. & Sabatini, D.M. Microarrays of cells expressing defined cDNAs. *Nature* **411**, 107–110 (2001).
63. Tramier, M. *et al.* Homo-FRET versus hetero-FRET to probe homodimers in living cells. *Methods Enzymol.* **360**, 580–597 (2003).
64. Krishnan, R.V., Varma, R. & Mayor, S. Fluorescence methods to probe nanometer-scale organization of molecules in living cell membranes. *J. Fluoresc.* **11**, 211–226 (2001).
65. Wallrabe, H., Elangovan, M.A.B., Periasamy, A. & Barroso, M. Confocal FRET microscopy to measure clustering of ligand–receptor complexes in endocytic membranes. *Biophys. J.* **85**, 559–571 (2003).
66. Garini, Y., Katzir, N., Cabib, D. & Buckwald, R.A. Spectral bio-imaging in *Fluorescence Imaging Spectroscopy and Microscopy* (eds. Wang, X.F. & Herman, B.) 87–124 (John Wiley & Sons, New York, 1996).
67. Jares-Erijman, E. & Jovin, T.M. Determination of DNA helical handedness by fluorescence resonance energy transfer. *J. Mol. Biol.* **257**, 597–617 (1996).
68. Hiraoka, Y., Shimi, T. & Haraguchi, T. Multispectral imaging fluorescence microscopy for living cells. *Cell Struct. Funct.* **27**, 367–374 (2002).
69. Elangovan, M. *et al.* Characterization of one- and two-photon excitation fluorescence resonance energy transfer microscopy. *Methods* **29**, 58–73 (2003).
70. Selvin, P.R. Principles and biophysical applications of lanthanide-based probes. *Annu. Rev. Biophys. Biomol. Struct.* **31**, 275–302 (2002).
71. Xu, Y., Piston, D.W. & Johnson, C.H. A bioluminescence resonance energy transfer (BRET) system: application to interacting circadian clock proteins. *Proc. Natl. Acad. Sci. USA* **96**, 151–156 (1999).
72. Gadella, T.W.J. Jr., van der Krogt, G.N.M. & Bisseling, T. GFP-based FRET microscopy in living plant cells. *Trends Plant Sci.* **4**, 287–291 (1999).
73. Schönle, A., Glatz, M. & Hell, S.W. Four-dimensional multiphoton microscopy with time-correlated single-photon counting. *Appl. Opt.* **39**, 6306–6311 (2000).
74. Yu, W., Mantulin, W.W. & Gratton, E. Fluorescence lifetime imaging: new microscopy techniques in *Emerging Tools for Single Cell Analysis* (eds. Durack, G. & Robinson, J.P.) 139–173 (Wiley-Liss, New York, 2000).
75. Harpur, A.G., Wouters, F.S. & Bastiaens, P.I.H. Imaging FRET between spectrally similar GFP molecules in single cells. *Nat. Biotechnol.* **19**, 167–169 (2001).
76. Carlsson, K. & Philip, J. Theoretical investigation of the signal-to-noise-ratio for different fluorescence lifetime imaging techniques. *SPIE Proc.* **4622**, 70–78 (2002).
77. Elson, D.S. *et al.* Wide-field fluorescence lifetime imaging with optical sectioning and spectral resolution applied to biological samples. *J. Mod. Opt.* **49**, 985–995 (2002).
78. Gerritsen, H.C., Asselbergs, M.A.H., Agronskaia, A.V. & van Sark, W.G.J.H.M. Fluorescence lifetime imaging in scanning microscopes: acquisition speed, photon economy and lifetime resolution. *J. Microsc.* **206**, 218–224 (2002).
79. Hanley, Q.S., Arndt-Jovin, D.J. & Jovin, T.M. Spectrally resolved fluorescence lifetime imaging microscopy. *Appl. Spectrosc.* **56**, 155–166 (2002).
80. Calleja, V. *et al.* Monitoring conformational changes of proteins in cells by fluorescence lifetime imaging microscopy. *Biochem. J.* **372**, 33–40 (2003).
81. Knemeyer, J.-P., Herten, D.-P. & Sauer, M. Detection and identification of single molecules in living cells using spectrally resolved fluorescence lifetime imaging microscopy. *Anal. Chem.* **75**, 2147–2153 (2003).
82. Krishnan, R.V., Saitoh, H., Terada, H., Centonze, V.E. & Herman, B. Development of a multiphoton fluorescence lifetime imaging microscopy (FLIM) system using a streak camera. *Rev. Sci. Instrum.* **74**, 2714–2721 (2003).
83. Siegel, J. *et al.* Wide-field time-resolved fluorescence anisotropy imaging (TR-FAIM): imaging the rotational mobility of a fluorophore. *Rev. Sci. Instrum.* **74** (2003).
84. Jovin, T.M. & Arndt-Jovin, D.J. Luminescence digital imaging microscopy. *Annu. Rev. Biophys. Biophys. Chem.* **18**, 271–308 (1989).
85. Young, R.M., Arnette, J.K., Roess, D.A. & Barisas, B.G. Quantitation of fluorescence energy transfer between cell surface proteins via fluorescence donor photobleaching kinetics. *Biophys. J.* **67**, 881–888 (1994).
86. Lippincott-Schwartz, J., Snapp, E. & Kenworthy, A. Studying protein dynamics in living cells. *Nat. Rev. Mol. Cell Biol.* **2**, 444–456 (2001).
87. Kenworthy, A.K. Imaging protein–protein interactions using fluorescence resonance energy transfer microscopy. *Methods* **24**, 289–296 (2001).
88. Matkó, J., Jenei, A., Matyus, L., Ameloot, M. & Damjanovich, S. Mapping of cell surface protein-patterns by combined fluorescence anisotropy and energy transfer measurements. *J. Photochem. Photobiol. B* **19**, 71–73 (1993).
89. Runnels, L.W. & Scarlata, S.F. Theory and application of fluorescence homotransfer to melittin oligomerization. *Biophys. J.* **69**, 1569–1583 (1995).
90. Yan, Y. & Marriott, G. Fluorescence resonance energy transfer imaging microscopy and fluorescence polarization imaging microscopy. *Methods Enzymol.* **360**, 561–580 (2003).
91. Buehler, C., Dong, C.Y., So, P.T.C., French, T. & Gratton, E. Time-resolved polarization imaging by pump-probe (stimulated emission) fluorescence microscopy. *Biophys. J.* **79**, 536–549 (2000).
92. Mathies, R.A., Peck, K. & Stryer, L. Optimization of high-sensitivity fluorescence detection. *Anal. Chem.* **62**, 1786–1791 (1990).
93. Dunn, G.A., Dobbie, I.M., Monypenny, J., Holt, M.R. & Zicha, D. Fluorescence localization after photobleaching (FLAP): a new method for studying protein dynamics in living cells. *J. Microsc.* **205**, 109–112 (2002).